

# Population models of farmed abalone *Haliotis diversicolor supertexta* exposed to waterborne zinc

Bo-Ching Chen<sup>a</sup>, Chung-Min Liao<sup>b,\*</sup>

<sup>a</sup>Department of Post-Modern Agriculture, Mingdao University, Changhua 52345, Taiwan ROC

<sup>b</sup>Department of Bioenvironmental Systems Engineering, National Taiwan University, Taipei 10617, Taiwan ROC

Received 27 April 2004; received in revised form 15 August 2004; accepted 19 August 2004

## Abstract

A stage-classified demographic method was performed to investigate the effects of increased waterborne zinc (Zn) concentrations on the population dynamics of abalone *Haliotis diversicolor supertexta*. We reanalyzed the results of a 7-day acute and a 28-day chronic toxicity bioassays to examine the survival and growth performances when exposing abalone to different levels of zinc stresses. An energy-based biological approach was adopted to model the effects of zinc on fecundity. These data provided stage-specific schedules of vital rates that were used to parameterize a projection matrix model for abalone. Simulations were carried out to produce temporal population abundance changes under seven exposure scenarios including a control group and six treated cohorts ranged from 0.03 to 1 mg l<sup>-1</sup> Zn. Model manipulations indicated that a reduction of individual growth rate was observed at an exposed Zn concentration greater than 0.12 mg l<sup>-1</sup>, whereas the significant influence of survivorship was occurred until the Zn concentration reached 0.25 mg l<sup>-1</sup>. For all treatments, Zn induced a slight decrease in fecundity. The asymptotic population growth rate decreased from  $\lambda=1.00$  for the control group to  $\lambda=0.9968$  for abalone population exposed to 1 mg l<sup>-1</sup> Zn, indicating a potential risk of population intrinsic growth rates for abalone exposed to higher levels of waterborne Zn. These findings provide a pivotal effort for setting of the ambient water quality criterion for protecting the aquacultural species.

© 2004 Elsevier B.V. All rights reserved.

**Keywords:** Ecotoxicology; Demography; Population dynamics; Zinc; Abalone

\* Corresponding author. Tel.: +886 2 2363 4512; fax: +886 2 2362 6433.

E-mail address: [cmliao@ntu.edu.tw](mailto:cmliao@ntu.edu.tw) (C.-M. Liao).

## 1. Introduction

From an ecotoxicological perspective, toxic substances may exert adverse effects at the individual, population, community and ecosystem level (Kramarz and Laskowski, 1997; Kammenga and Laskowski, 2000). All potential risks associated with toxic effects from the individual to the ecosystem should therefore be assessed while developing the ambient water quality criterion for protection of aquatic species. At present, however, most of the effect assessment of toxicants that can be found in the literature focus on convenient endpoints, such as the median lethal concentration ( $LC_{50}$ ) from the acute test and/or the no-observed-effect-concentration (NOEC) from the chronic test, handling in terms of individual-level variables instead of those at higher levels (Grist et al., 2003; Ducrot et al., 2004). Consequently, one of the major challenges in current ecotoxicology is to provide a better understanding of potential effects of toxicants on natural populations and ecosystems by using data extracted from traditional toxicity bioassays in laboratory (Chaumot et al., 2003; Eggen et al., 2004).

A rich body of ecotoxicological work today aims to develop mathematical tools for upscaling of individual contaminant effects to population levels by using demographic models to meet the need (Simas et al., 2001; Kuhn et al., 2002). The demographic models, based on the vital rates in the context of the whole life cycle of individuals, can mainly be classified into three approaches differing in whether time and stage are continuous or discrete variables (Caswell, 2001). The most popular one is the matrix population model characterized by a population projection matrix (referred to as Leslie matrix) to project the population from time  $t$  to time  $t+1$  (Caswell, 2001). A stage-classified matrix model classifies individuals by an appropriate set of real biological stages as of unequal duration (Van Straalen and Kammenga, 1998). Due to its biological relevance, stage-classified matrix model has been widely applied in addressing the relationships among toxicants, individual life-table response data and population growth rate (Klok and deRoos, 1996; Simas et al., 2001).

Many marine mollusks and algae, due to their wide distributions, extensive populations, sedentary nature and ability to accumulate contaminants, have been suggested as ideal bioindicators of heavy metal contamination in aquatic ecosystems (Liao and Lin, 2001). Abalone are common gastropod mollusks that inhabit the coastal reefs in tropical and subtropical areas (Chen and Lee, 1999). The herbivorous gastropod, *Haliotis diversicolor supertexta*, is the most abundant abalone species in Taiwan. *H. diversicolor supertexta* prefers red algae, *G. tenuistipitata* var. *liui*, which yield the best growth of the abalone (Chen and Lee, 1999). The fisheries and aquaculture of these two species are commercially important for their delicacy and high market value in Taiwan (Liao and Lin, 2001; Liao et al., 2004).

Zinc (Zn) is an essential micronutrient found at high levels in the algae and in the tissues of fish/shellfish (Hogstrand et al., 1998; Liao et al., 2002a). Zn is available to abalone from both the dissolved phase (e.g., gill uptake) and the diet (e.g., algae ingestion) (Tsai et al., 2004). This transition metal is responsible for many biological functions and it stabilizes biological molecules and structures in organisms (Muysen and Janssen, 2002; Mauri et al., 2003). If waterborne Zn levels are elevated, however,

toxicity can occur and have severe effects on the health of *H. diversicolor supertexta*, which will reduce market prices and cause closure of abalone farms. Previous investigations indicated that Zn was detected in many rivers and that maximum Zn concentrations in contaminated aquacultural waters were reported to range from 60 to 130  $\mu\text{g l}^{-1}$  in different areas of Taiwan (Lee et al., 1996). At these levels, Zn specifically disrupts calcium uptake by the gills of fish (Hogstrand et al., 1998), leading to hypocalcemia, which may end with the death of the fish within a few days, depending on the Zn concentration.

Liao et al. (2002a) and Tsai et al. (2004) have conducted a 7-day acute and a 28-day chronic toxicity bioassays to determine, respectively, the  $\text{LC}_{50}$  and the NOEC of abalone *H. diversicolor supertexta* exposed to Zn at different exposure concentrations. Both acute and chronic endpoints (i.e., mortality rate and growth rate) were also examined to investigate the toxic effects of Zn on individual abalone. A probabilistic risk assessment of abalone exposed to waterborne Zn further indicated that a high individual growth risk in some aquacultural ponds of Taiwan is alarming (Liao and Ling, 2004). Compared with these individual endpoints, however, population-level effects are of particular concerns for the development of ambient water quality criteria due to their superior importance for ecological functions (U.S. EPA, 1991). From this point of view, the data obtained from traditional toxicity tests should be incorporated into demographic model to predict effects of Zn on abalone population.

The purpose of this study is to perform a stage-classified demographic method to investigate the effects of increased concentrations of waterborne Zn on the population dynamics of abalone *H. diversicolor supertexta*. Data obtained from our previous toxicity bioassays were reanalyzed to reconstruct dose–response profiles and to examine the survival and growth performances. An energy-based biological approach was also adopted to model the effects of Zn on reproductive values for each age class. These data provided stage-specific schedules of vital rates that were used to parameterize a projection matrix model for abalone. Simulations were carried out to produce population abundance changes over time under different exposure scenarios. Asymptotic population growth rates were also estimated from matrix population models to further provide an ecotoxicological endpoint at the population level.

## 2. Materials and methods

### 2.1. Stage-classified demographic model

To develop the stage-classified demographic model of abalone exposed to waterborne Zn, a life cycle graph which can completely describes the dynamic processes of all relevant stages of the life history of abalone should be formulated in advance. We divided the life cycle of abalone into four developmental phases, i.e., the post-larvae, juvenile, sub-adult, and the adult stage, based on the shell lengths of abalone as suggested by Chen and Lee (1999) (Fig. 1), indicating that the duration of each life stage of abalone is estimated to be 50, 300, 400, and 500 days, respectively, yielding a life span of 1250 days.

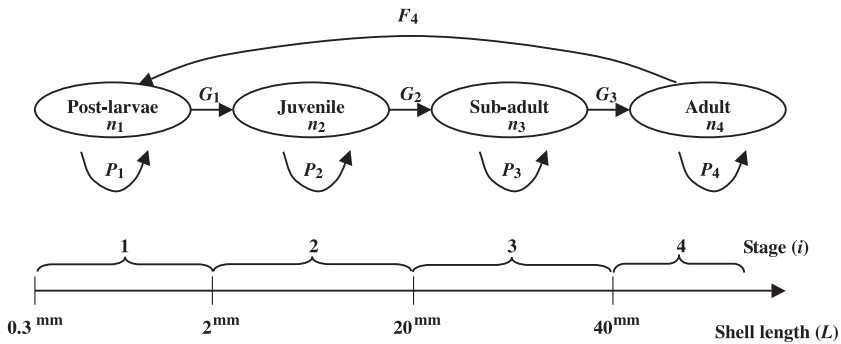


Fig. 1. A four-stage life cycle graph of an individual abalone *H. diversicolor supertexta*. The meanings of the symbols are given in the text.

The abundances in each stage after a projection interval from  $t$  to  $t+1$  can be expressed as (Caswell, 2001) (Fig. 1)

$$\begin{aligned} n_1(t+1) &= P_1 n_1(t) + F_4 n_4(t), \\ n_2(t+1) &= P_2 n_2(t) + G_1 n_1(t), \\ n_3(t+1) &= P_3 n_3(t) + G_2 n_2(t), \\ n_4(t+1) &= P_4 n_4(t) + G_3 n_3(t), \end{aligned} \quad (1)$$

where  $n_i(t)$  is the numbers of abalone in stage  $i$  at time  $t$ ,  $P_i$  is the probability of surviving and staying in stage  $i$ ,  $G_i$  is the probability of surviving and growing from stage  $i$  to stage  $i+1$ , and  $F_4$  is the *per capita* fertility of stage 4 within each projection interval. Eq. (1) can be reduced to a vector-matrix representation

$$\begin{Bmatrix} n_1 \\ n_2 \\ n_3 \\ n_4 \end{Bmatrix} (t+1) = \begin{bmatrix} P_1 & 0 & 0 & F_4 \\ G_1 & P_2 & 0 & 0 \\ 0 & G_2 & P_3 & 0 \\ 0 & 0 & G_3 & P_4 \end{bmatrix} \begin{Bmatrix} n_1 \\ n_2 \\ n_3 \\ n_4 \end{Bmatrix} (t), \quad (2)$$

and compactly expressed as

$$\{n(t+1)\} = [A]\{n(t)\}. \quad (3)$$

The matrix  $[A]$  in Eq. (3), usually referred to as the population projection matrix, includes positive entries on the diagonal corresponding to individuals remaining in the same size class as well as on the off-diagonal (Caswell, 2001). Matrix models combine the survival and fecundity of individuals (the matrix elements) to estimate an asymptotic population growth rate,  $\lambda$  (the dominant eigenvalue of  $[A]$ ), reflecting the temporal trend in population abundance (Caswell, 2001; Chaumot et al., 2003). When  $\lambda$  exceeds 1.00, the population is projected to increase over time, whereas the population is projected to decline when  $\lambda$  is less than 1.00. The elements  $P_i$ ,  $G_i$ , and  $F_4$  of the population projection matrix  $[A]$  are referred to as the life cycle parameters or transition probabilities. The

transition probabilities  $P_i$  and  $G_i$  can be formulated in terms of the stage-specific vital rates as (Caswell, 2001)

$$P_i = \sigma_i(1 - \gamma_i), \quad (4)$$

$$G_i = \sigma_i\gamma_i, \quad (5)$$

where  $\sigma_i$  and  $\gamma_i$  denote the stage-specific vital rates of survival and growth probabilities ( $\text{day}^{-1}$ ), respectively. In accordance with the exposure conditions of previous chronic bioassays (Tsai et al., 2004), seven scenarios, with dissolved Zn concentrations of 0, 0.03, 0.06, 0.12, 0.25, 0.5, and 1  $\mu\text{g ml}^{-1}$  (designated as scenarios A to G, respectively), were used to simulate population dynamics of abalone under different levels of environmental Zn stresses. In subsequent sections, we will describe the methods to determine the stage-specific vital rates of individual abalone exposed to different levels of waterborne Zn.

## 2.2. Individual growth probabilities, $\gamma_i$

Stage-specific growth rates under no environmental Zn stress (Scenario A) can be calculated by fitting abalone shell length data of each developmental stage obtained from literatures to an exponential growth model (Liao et al., 2004)

$$\ln L = c + gt, \quad (6)$$

where  $L$  refers to the abalone shell length at culture time  $t$  in days (cm),  $c$  is a constant, and  $g$  is the growth rate ( $\text{day}^{-1}$ ).

The relationships between growth coefficient and Zn concentration obtained from Tsai et al. (2004) were applied to determine the stage-specific growth rates of abalone under Zn stresses for scenarios B to G. With the assumption that all individuals within each stage have identical growth rates, the individual growth probabilities  $\gamma_i$  can be expressed analogously to the biological interpretation proposed by Van Straalen and Kammenga (1998)

$$\gamma_i = \frac{g_i T}{d_i}, \quad (7)$$

where  $g_i$  represents the growth rate of abalone in stage  $i$  ( $\text{day}^{-1}$ ),  $T$  is the projection interval (day), and  $d_i$  is the duration of stage  $i$  (day).

## 2.3. Survival probabilities, $\sigma_i$

To formulate the intrinsic survival rate of abalone, we adopted a survival curve for a population under natural circumstances proposed by Klok and deRoos (1996)

$$S(t) = \left( \frac{(1 - at)}{1 + bt} \right)^k, \quad (8)$$

where  $S(t)$  is the intrinsic survival rate of abalone at age  $t$ , and  $a$ ,  $b$ , and  $k$  are constants. Klok and deRoos (1996) indicated that  $a$  and  $b$  are biological parameters and are inversely proportion to the maximum life span of the considered species. Consequently, with a

maximum life span of abalone of 1250 days, parameter values of  $a$  and  $b$  associated with abalone were equal to 0.0008 and 0.011, respectively. By introducing the survival data of abalone proposed by Chen and Lee (1999) into Eq. (8),  $k$  value was estimated as 0.194. The intrinsic survival probability of abalone in stage  $i$  during a projection interval ( $\sigma_{i,0}$ ) can then be calculated as

$$\sigma_{i,0} = \frac{S(t+T) - S(t)}{T}. \quad (9)$$

Prior to determination of stage-specific mortality rates for abalone subject to waterborne Zn concentration, we employed a pharmacodynamic model developed by Liao et al. (2002a)

$$M(t) = \frac{M_{\max} \times C_m^n(t)}{C_{L,50}^n(t) + C_m^n(t)}, \quad (10)$$

where  $M(t)$  is the time-dependent mortality of abalone,  $M_{\max}$  is abalone maximum mortality,  $C_{L,50}(t)$  represents the internal body burden of Zn in abalone that causes 50% mortality ( $\mu\text{g g}^{-1}$ ),  $C_m(t)$  is the whole-body burden of Zn in abalone at time  $t$  ( $\mu\text{g g}^{-1}$ ), and  $n$  is the Hill coefficient.

Based on the toxicity test, however, mortality functions were estimated from observed mortality percentages in exposure regimes in which mortality was an increasing function of the Zn concentration in water. Therefore, assuming the exposure time approaches infinity, Eq. (10) becomes

$$M(t) = \frac{M_{\max} \times C_m^n(t)}{(BCF \times LC_{50}(\infty))^n + C_m^n(t)}, \quad (11)$$

where BCF is the bioconcentration factor of abalone for Zn and  $LC_{50\infty}$  is the incipient median lethal concentration of Zn in water ( $\mu\text{g ml}^{-1}$ ).

Zinc is accumulated in abalone both by dietary (i.e., red algae, *G. tenuistipitata* var. *liui*) and nondietary (i.e., water source) routes. If the dissolved Zn concentration in water is assumed to be constant, whereas the Zn concentration in algae is assumed to vary with time, the temporal change of Zn concentration in abalone could be modeled using the first-order one-compartment model

$$\frac{dC_m(t)}{dt} = \alpha f C_a(t) + k_1 C_w - (k_2 + g) C_m(t), \quad (12)$$

where  $C_w$  is the dissolved Zn concentration in water ( $\mu\text{g ml}^{-1}$ ),  $C_a(t)$  is the time-dependent Zn concentration in algae ( $\mu\text{g g}^{-1}$ ),  $\alpha$  is the assimilation efficiency of abalone,  $f$  is the abalone grazing rate ( $\text{g g}^{-1} \text{ day}^{-1}$ ),  $k_1$  is the abalone uptake rate of Zn ( $\text{ml g}^{-1} \text{ day}^{-1}$ ), and  $k_2$  is the abalone depuration rate ( $\text{day}^{-1}$ ). Assuming that the initial Zn concentration was equal to zero in algae,  $C_a(t)$  can be expressed as (Liao et al., 2004)

$$C_a(t) = BCF_a C_w (1 - e^{-(k_{2a} + g_a)t}), \quad (13)$$

where  $BCF_a$  is the bioconcentration factor of *G. tenuistipitata* var. *liui* for Zn,  $k_{2a}$  is the algae depuration rate ( $\text{day}^{-1}$ ), and  $g_a$  is the algae growth rate ( $\text{day}^{-1}$ ).

The solution to Eq. (12) when Zn concentration in algae is modeled by Eq. (13) is given by (Gross-Sorokin et al., 2003)

$$C_m(t) = \left[ \frac{\alpha f G_a}{B_a - B_m} \right] (e^{-B_m t} - e^{-B_a t}) + \left[ \frac{\alpha f G_a}{B_m} \right] (1 - e^{-B_m t}) + G_m (1 - e^{-B_m t}), \quad (14)$$

where  $G_m = \text{BCF } C_w$ ,  $G_a = \text{BCF}_a C_w$ ,  $B_m = k_2 + g$ , and  $B_a = k_{2a} + g_a$ . All parameters revealed in Eqs. (11) and (14) can be obtained from our previous studies based on the acute toxicity bioassay of abalone and algae exposed to waterborne Zn (Liao et al., 2002a, 2004). For a given stage and waterborne Zn concentration, the mortality rates of abalone ( $M_i(t)$ ) can be calculated by substituting  $C_m(t)$  of Eq. (14) in the parameterization of Eq. (11). The survival probability of abalone of stage  $i$  at time  $t$  under different exposure scenarios can be determined by combining Eqs. (9) and (11) as

$$\sigma_i = \sigma_{i,0} (1 - M_i(t)). \quad (15)$$

#### 2.4. Reproduction rate, $F_4$

The reproduction rate in stage 4 of abalone under no environmental Zn stress was determined through a reproductive model proposed by Simas et al. (2001) as

$$F_4 = F_e E F_m, \quad (16)$$

where  $F_e$  is the number of eggs per mature female per unit time ( $\text{day}^{-1}$ ) and is referred to as fecundity,  $E$  is the egg eclosion rate, and  $F_m$  is the percentage of mature female in stage 4. The fecundity, however, will decrease once the exposure concentration exceeds the chronic endpoint, NOEC. We adopted an energy-based biological approach developed by Ducrot et al. (2004) to model the effects of Zn on abalone fecundity,

$$F_e = F_{e,0} [1 - h(C_w - \text{NOEC})], \quad (17)$$

where  $F_{e,0}$  is the control fecundity of abalone and  $h$  is the level of toxicity of Zn for abalone ( $\text{kg mg}^{-1}$ ). The control fecundity of abalone ( $F_{e,0}$ ) was available from the PondFX Aquatic Life Database ([www.ent.orst.edu/PondFX](http://www.ent.orst.edu/PondFX)) maintained by Oregon State University (Corvallis, OR, USA) and has a value of  $0.21 \text{ day}^{-1}$ . The level of toxicity of Zn for abalone ( $h$ ) was considered to have an order of magnitude of  $10^{-3}$  based on the mean value ranges suggested by Ducrot et al. (2004).

#### 2.5. Input parameters and model simulation

All parameters used to calculate the vital rates ( $\gamma_i$ ,  $\sigma_i$ ,  $F_4$ ) of individual abalone were summarized in Table 1. The experiments carried out by Liao et al. (2002a, 2004) and Tsai et al. (2004) were set to imitate the actual culture operations of abalone farms. Therefore, all parameters listed in Table 1 are obtained under comparable experimental conditions. To manipulate the simulation of stage-classified demographic model, a projection interval of 1 day was used. Caswell (2001) pointed out that the initial condition has no influence on the stable age distributions as well as population growth rate. Therefore, the initial number of abalone of each stage ( $n_1$ ,  $n_2$ ,  $n_3$ ,  $n_4$ ) was arbitrarily assumed to be 500, 0, 0, and 500,

Table 1

Parameters used to calculate the vital rates of abalone

Parameters	Values	Units	Sources
<i>Growth probabilities<sup>a</sup></i>			
$g_1$	$5.4 \times 10^{-2}$	day <sup>-1</sup>	Martinez-Ponce and Searcy-Bernal (1998)
$g_2$	$9.0 \times 10^{-3}$	day <sup>-1</sup>	Shepherd (1998)
$g_3$	$4.0 \times 10^{-3}$	day <sup>-1</sup>	Yang and Ting (1986)
$g_4$	$8.0 \times 10^{-4}$	day <sup>-1</sup>	Yang and Ting (1984)
<i>Survival probabilities</i>			
$n$	3.7	—	Liao et al. (2002a,b)
BCF	328.25	—	Liao et al. (2004)
BCF <sub>a</sub>	261	—	Liao et al. (2004)
$k_2$	0.024	day <sup>-1</sup>	Liao et al. (2004)
$k_{2a}$	0.811	day <sup>-1</sup>	Liao et al. (2004)
LC <sub>50</sub> ( $\infty$ )	1.17	$\mu\text{g ml}^{-1}$	Liao et al. (2002a,b)
$\alpha$	34.57	%	Liao et al. (2004)
$f$	0.25	$\text{g g}^{-1} \text{day}^{-1}$	Chen and Lee (1999)
$g_a$	0.038	day <sup>-1</sup>	Lee et al. (1996)
$M_{\text{max}}$	100	%	—
<i>Reproduction rate</i>			
$F_m$	50	%	—
$E$	3.1	%	Simas et al. (2001)
NOEC	0.06	$\mu\text{g ml}^{-1}$	Tsai et al. (2004)

<sup>a</sup> Natural growth rate of abalone calculated from Eq. (6) under no Zn stress.

respectively, yielding an initial population density of 1000 individuals per unit area. Model simulations and the determinations of asymptotic population growth rate under different scenarios were performed using the MATLAB<sup>®</sup> software (The Mathworks, MA, USA).

### 3. Results and discussion

#### 3.1. Effects of Zn on asymptotic population growth rate, $\lambda$

Incorporating survival and fecundity rates into population models reveals substantial differences in the asymptotic population growth rates ( $\lambda$ ) in each scenario. In order to know the effect of waterborne Zn concentration ( $C_w$ ) on the global population endpoint  $\lambda$ , we used  $d\lambda/dC_w$  to indicate the sensitivity of  $\lambda$  to changes in the Zn concentrations (Caswell, 2001). The  $d\lambda/dC_w$  value also reflects a measure for the change of the global growth response with higher concentrations, indicating the more drastically the response changes with higher concentrations.

Fig. 2A shows a reduction in the asymptotic population growth rate for increasing Zn concentrations. A reference value of  $\lambda=1.00$  was obtained for the asymptotic population rate in the absence of Zn concentration, indicating a stable population. Potential growths for the population ( $\lambda>1.00$ ) were shown at the Zn concentrations of 0.03 and 0.06  $\text{mg l}^{-1}$



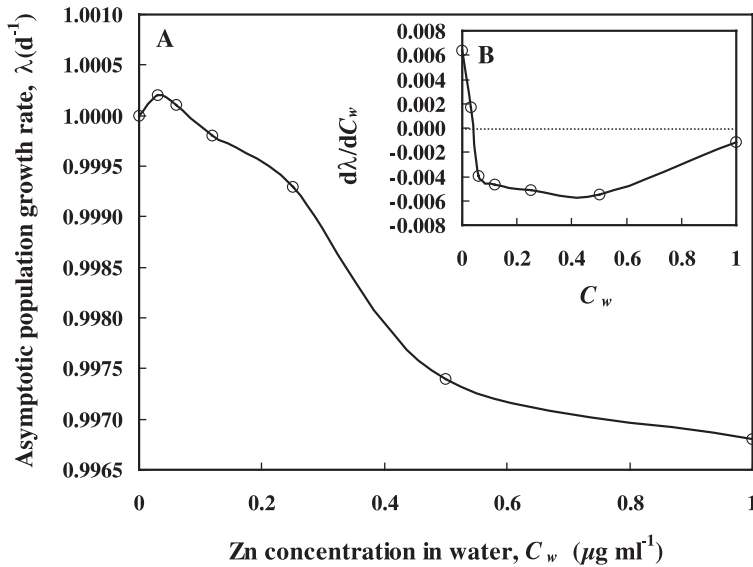


Fig. 2. Effects of increasing waterborne Zn concentrations on (A) the asymptotic population growth rates of abalone and (B) the sensitivities of the asymptotic population growth rates on abalone to different exposure scenarios.

due to the hormesis (Fig. 2A). Fig. 2A also demonstrates that the asymptotic population growth rate decreased from  $\lambda=1.00$  for the control group to  $\lambda=0.9968$  for abalone population exposed to  $1 \text{ mg l}^{-1}$  Zn, indicating a potential risk of population intrinsic growth rates for abalone exposed to higher levels of waterborne Zn.

The effect of waterborne Zn concentrations ranged from 0.12 to  $0.5 \text{ mg l}^{-1}$  has the significant reducing contribution on the asymptotic population growth rate  $\lambda$  (Fig. 2B), indicating that a reduction of global population growth rate was observed at an exposed Zn concentration greater than  $0.12 \text{ mg l}^{-1}$ , whereas the significant influence of population abundance was occurred until the Zn concentration reached  $0.5 \text{ mg l}^{-1}$ . A larger  $d\lambda/dC_w$  value means that small changes in concentration will have a big effect on the resulting global population endpoint  $\lambda$ . Differences in  $d\lambda/dC_w$  value reflect the different concentrations and the way they affect the long-term population growth rate.

### 3.2. Effect of Zn on individual growth rate and bioaccumulation of abalone

Individual growth rates of control abalone as well as treated ones all declined from an order of  $10^{-2}$  to  $10^{-4} \text{ day}^{-1}$  for larval and adult abalone, respectively (Fig. 3A,B). As Zn concentration increases, however, non-monotonic concentration–response curves were observed for all life stages of abalone (Fig. 3A,B). The highest growth rates were obtained at a Zn concentration of  $0.03 \mu\text{g ml}^{-1}$ , whereas the lowest values were appeared at  $0.5 \mu\text{g ml}^{-1}$ . The highest Zn concentration that did not have an inhibiting effect on abalone growth rate was  $0.06 \mu\text{g ml}^{-1}$ , yielding a NOEC of  $0.06 \mu\text{g ml}^{-1}$  and an LOEC (lowest-

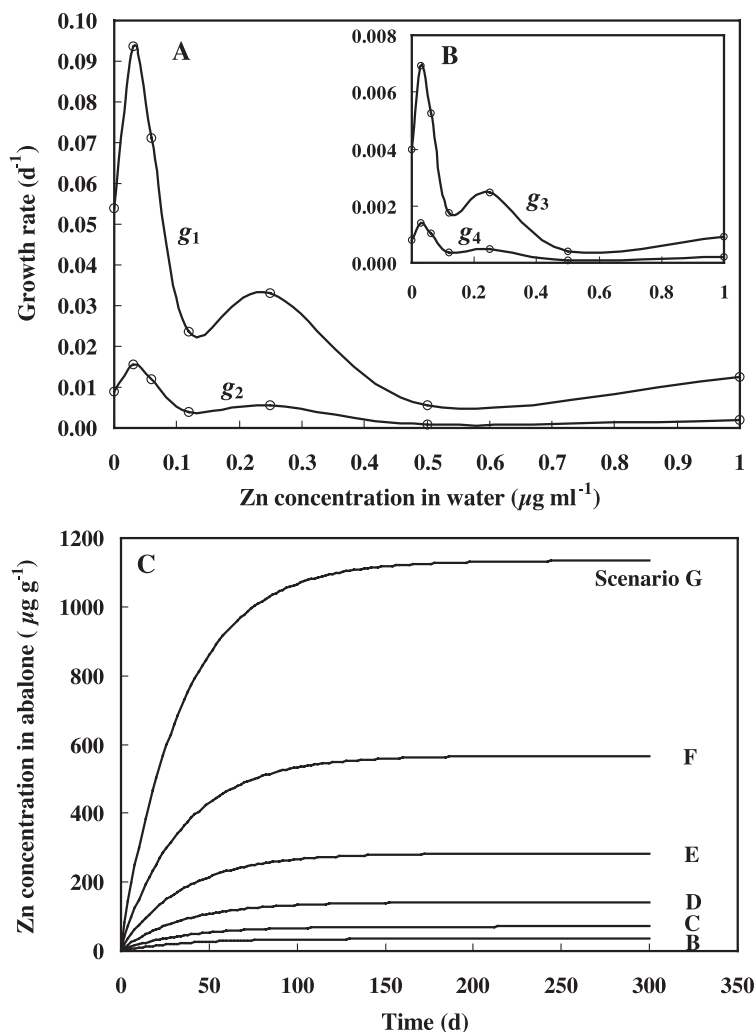


Fig. 3. Individual growth rates ( $g$ ) of abalone expose to different waterborne Zn concentrations for (A) stages 1 and 2 and (B) stages 3 and 4; and (C) predicted time-varying whole-body Zn concentrations of abalone under different exposure scenarios ranged from 0.03 to 1  $\mu\text{g Zn ml}^{-1}$  (scenarios B: 0.03, C: 0.06, D: 0.12, E: 0.25, F: 0.5, and G: 1  $\mu\text{g Zn ml}^{-1}$ ).

observed effect concentration) of 0.12  $\mu\text{g ml}^{-1}$  for the chronic endpoint of the designed exposure condition as determined by Tsai et al. (2004).

The dose–response curve for toxicant-influenced endpoint often conforms to either a linear or a threshold model (Renner, 2004). The phenomenon that a stimulatory effect, however, may be exhibited with exposure to low-dose toxicant rather than high-dose inhibition, usually referred to as “hormesis” has been receiving growing attentions (Kooijman, 1998; Renner, 2004). Calabrese and Baldwin (2003) developed a priori defined criteria to reassess numerous toxicological papers and demonstrated that the

hormetic responses are widely revealed in almost all species. Our results also confirmed that the growth rates of abalone are stimulated in 0.03 and 0.06  $\mu\text{g Zn ml}^{-1}$ .

Although the actual cause is largely unknown, some common features of hormesis have been identified. For the endpoint being growth, the hormetic dose–response curve usually takes an inverse U shape when exposing organisms to low doses of various toxic metals (Calabrese and Baldwin, 2003). In the present study, a biphasic, quasi-U shape dose–response curves were obtained for abalone exposed to waterborne Zn (Fig. 3A,B). Renner (2004) further indicated that the stimulatory responses were estimated to be 30% to 60% greater than with no hormetic dose, which was consistent with our results.

It has been generally recognized that several parameters including body weight, shell length, food conversion rate, condition index, and sexual maturation can be used while modeling growth of shellfishes (Appleyard and Dealteris, 2001). We fitted the exponential growth model to the experimental shell length data to estimate individual growth rates of abalone since the longest dimension of shell has been widely proposed to characterize growth for many mollusk and clam species (Appleyard and Dealteris, 2001; Liao et al., 2004). Steinarsson and Imsland (2003) studied the effect of size on growth of red abalone (*Haliotis rufescens*) and indicated that the maximum growth was inversely related to initial shell length of this species. Our results further supported that abalone exhibits an inverse relationship between size and growth rate.

The accumulated Zn concentrations in abalone for all scenarios increased rapidly during the first month and reached equilibrium after 150 days (Fig. 3C). The equilibrium whole-body burdens for abalone exposed to 0.03, 0.06, 0.12, 0.25, 0.5, and 1  $\mu\text{g ml}^{-1}$  waterborne Zn were, respectively, 35.4, 70.9, 141.7, 283.4, 566.8, and 1133.6  $\mu\text{g g}^{-1}$  (Fig. 3C).

When referring to the bioaccumulation of chemical compounds in aquatic organisms, both dietary and soluble sources should be taken into consideration. It is generally recognized that trophic transfer of metals is an important pathway for metal accumulation in marine invertebrates and fishes (Wang and Ke, 2002; Liao et al., 2002b,2004). Liao et al. (2002a) simulated whole-body burdens for abalone and an equilibrium value of 166.6  $\mu\text{g g}^{-1}$  was obtained when exposing abalone to 1  $\mu\text{g ml}^{-1}$  waterborne Zn, indicating a much lower equilibrium value compared to that obtained in the present study (1133.6  $\mu\text{g g}^{-1}$ ). This result reflects a significant contribution of Zn from the dietary source.

Generally, the metal concentrations in the food sources on which the animals preyed were assumed constants to simplify the solution of the bioaccumulation model. For different stages of abalone, however, the consideration of time-varying dietary Zn concentration seemed more reasonable due to its crucial influence on bioaccumulation. In the present study, we employed a first-order one-compartment bioaccumulation model accounting for accumulation from both food and water was employed to predict the overall Zn accumulation in abalone in that the time-varying concentrations of algae were considered (i.e., Eq. (13)) to make an exhaustive inspection for modeling dietary Zn uptake by abalone.

### 3.3. Survivorship and fertility

Fig. 4A depicts a survival curve for abalone under natural circumstances, whereas the stage-specific survival proportions for abalone subject to waterborne Zn concentrations

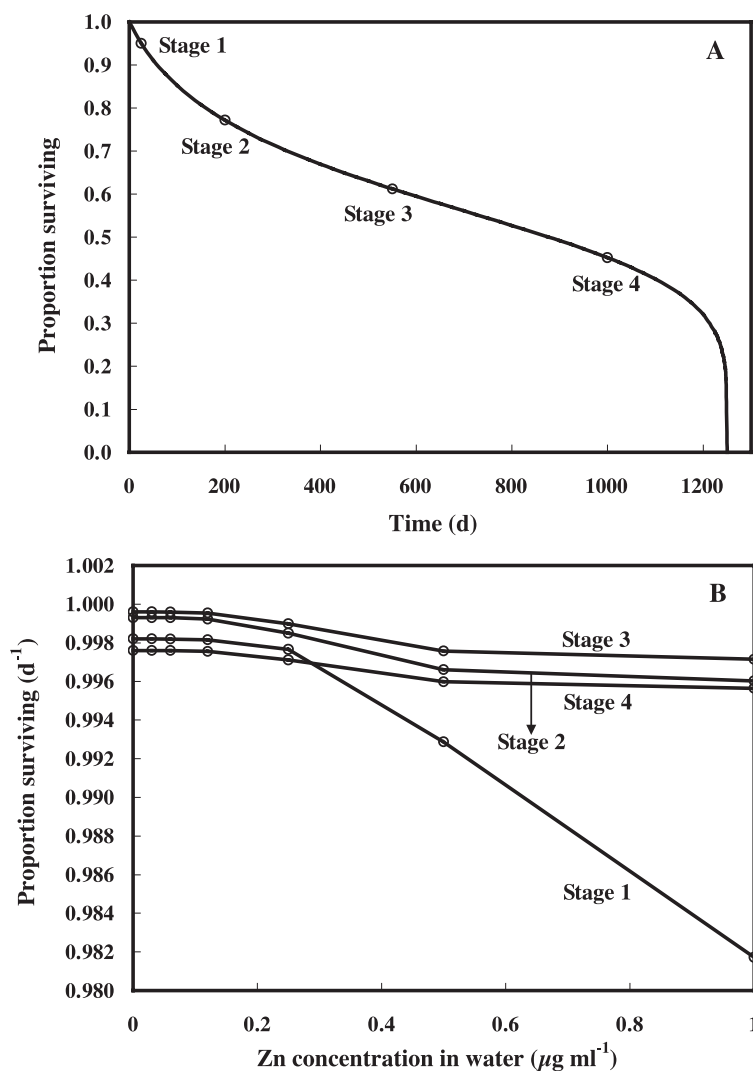


Fig. 4. Stage-specific survival proportions for (A) abalone under natural circumstances and (B) abalone subject to different waterborne Zn concentrations.

were presented in Fig. 4B. These survival curves were used to parameterize the daily-basis survival probabilities ( $\sigma_i$ ) of the stage-classified projection matrix model for abalone.

Shepherd (1998) demonstrated that the natural survival rates of abalone for stages 1 to 4 according to our classification are 0.977, 0.9991, 0.9994, and 0.9973 day<sup>-1</sup>, respectively. Comparing these values with survival rates of the control group obtained from Fig. 4A (0.9982, 0.9993, 0.9996, and 0.9976 day<sup>-1</sup>, respectively.), it is evidenced that the survival equation (Eq. (8)) successfully models the stage-specific survival rates of abalone under natural circumstances except for that of stage 1. This discrepancy may be resulted from the

fact that the predators of larval abalone in the field, such as crabs and wrasses, were not considered in our model (Shepherd, 1998).

Significant changes on abalone survivorship occurred when the waterborne Zn concentrations exceeded  $0.25 \mu\text{g ml}^{-1}$  for all life stages (Fig. 4B). For stages 2, 3, and 4, there were enough exposure durations for the Zn concentrations to accumulate in abalone since the equilibriums were reached after 150 days (Fig. 3C). The similar survival profiles for these stages were therefore obtained since identical whole-body concentrations of Zn were accumulated in abalone. Liao et al. (2002a) suggested that Zn is lethal to *H. diversicolor supertexta* at concentrations larger than  $1 \mu\text{g ml}^{-1}$ . For the present results, however, a potential risk of lethality for larval abalone revealed when waterborne Zn concentration exceeds  $0.5 \mu\text{g ml}^{-1}$  due to additional Zn accumulation from dietary route.

We applied an energy-based biological approach to model the effects of Zn on abalone fecundity. Due to the mathematical characteristics of Eq. (17), abalone fecundity will decrease linearly once the exposure Zn concentration exceeds the NOEC. The resulting value of reproduction rate,  $F_4$ , declined from  $3.25 \times 10^{-3}$  to  $3.22 \times 10^{-3} \text{ day}^{-1}$  for abalone of Scenarios A (the control group) and G (the treated group with highest exposure concentration), respectively. It should be noted that an average, daily time interval birthflow was used for model simulation. Consequently, a slight change in reproduction rate may result in a tremendous influence on the simulation result (Grist et al., 2003).

### 3.4. Population abundance

The temporal changes of stage-specific and overall population abundances of abalone exposed to different scenarios of waterborne Zn were presented in Fig. 5, whereas the concentration–response profile of abalone population after a 5-year simulation was given in Fig. 6 in that the simulation time period was determined from a pre-analysis for the control population to reach its stable age distribution.

The abundances of abalone in each life stage for Scenario A (the control group) all approach stable after 5 years, with numbers of 34, 184, 360, and 404 for larval, juvenile, sub-adult, and adult abalone, respectively (Fig. 5). The differences of numbers of abalone were mainly due to the corresponding span of age for each stage. For stages 1 and 4 of the control group, the stable distribution occurred within 1 year, whereas it spent nearly 2 years to reach stabilities for stages 2 and 3. Such a difference may be due to the selection of initial conditions of model simulation. Laskowski (2000) showed that large differences in predicted extinction time could be caused solely by the initial age structure of a population. Caswell (2001) also indicated that the time to stability was largely affected by the initial conditions. The stable age distributions, however, were proposed to stay unchanged of different initial conditions.

In view of Figs. 5 and 6, the treated groups can further be subdivided into three subgroups according to the ultimate fates of abalone population after the 5-year simulation. The reductions in population abundance for Scenarios B and C after 5-year exposures were negative, indicating positive population growth rates for these two scenarios (Fig. 6). For Scenarios D and E, the population abundances decreased slowly during the simulation period, indicating extinction risks when abalone exposed to waterborne Zn at a concentration larger than  $0.12 \mu\text{g ml}^{-1}$ , whereas for Scenarios F and G,

the population abundances of abalone declined rapidly and were extinct within 5 years (Fig. 6).

Laskowski and Hopkin (1996) studied the effects of four metals (Zn, Cu, Pb, and Cd) on fitness in snails and concluded that the population of snails may be decline at high metal concentrations in food. Similar results were obtained by other research works in which the demographic methods were performed to study the population effects of some

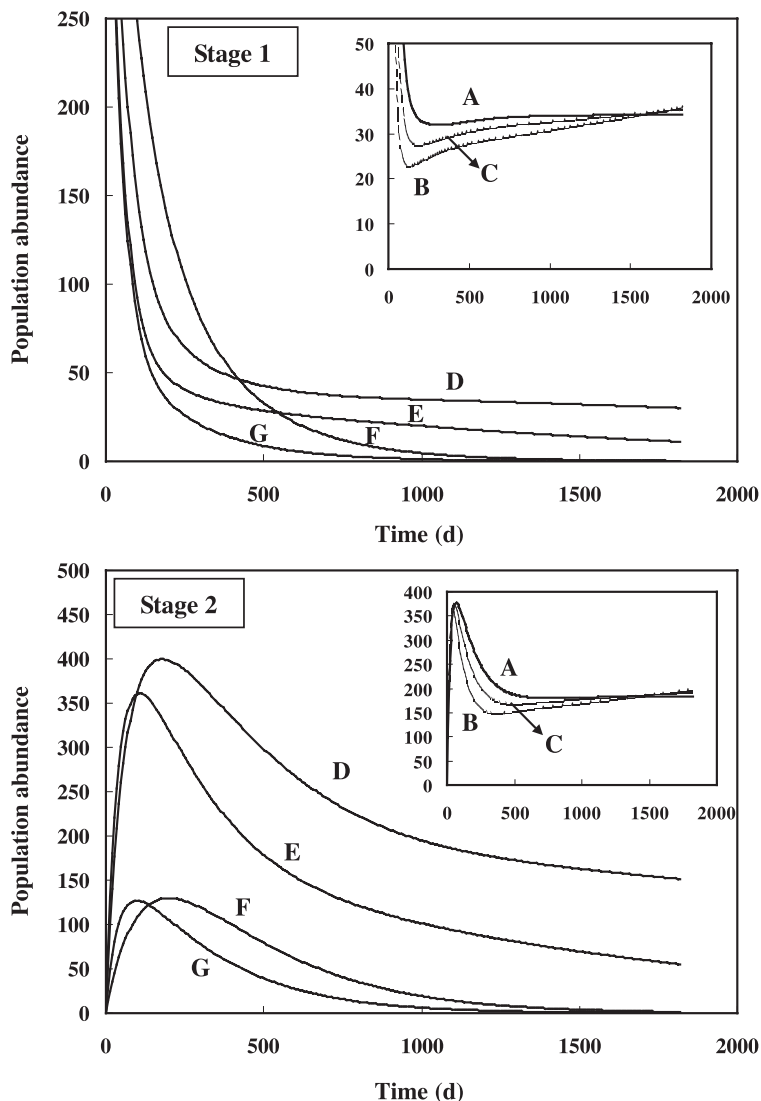


Fig. 5. Temporal changes of life-stages 1 to 4 and overall population abundances of abalone exposed to different scenarios of waterborne Zn as of scenarios A:0, B: 0.03, C: 0.06, D: 0.12, E: 0.25, F: 0.5, and G:  $1 \mu\text{g Zn ml}^{-1}$ .

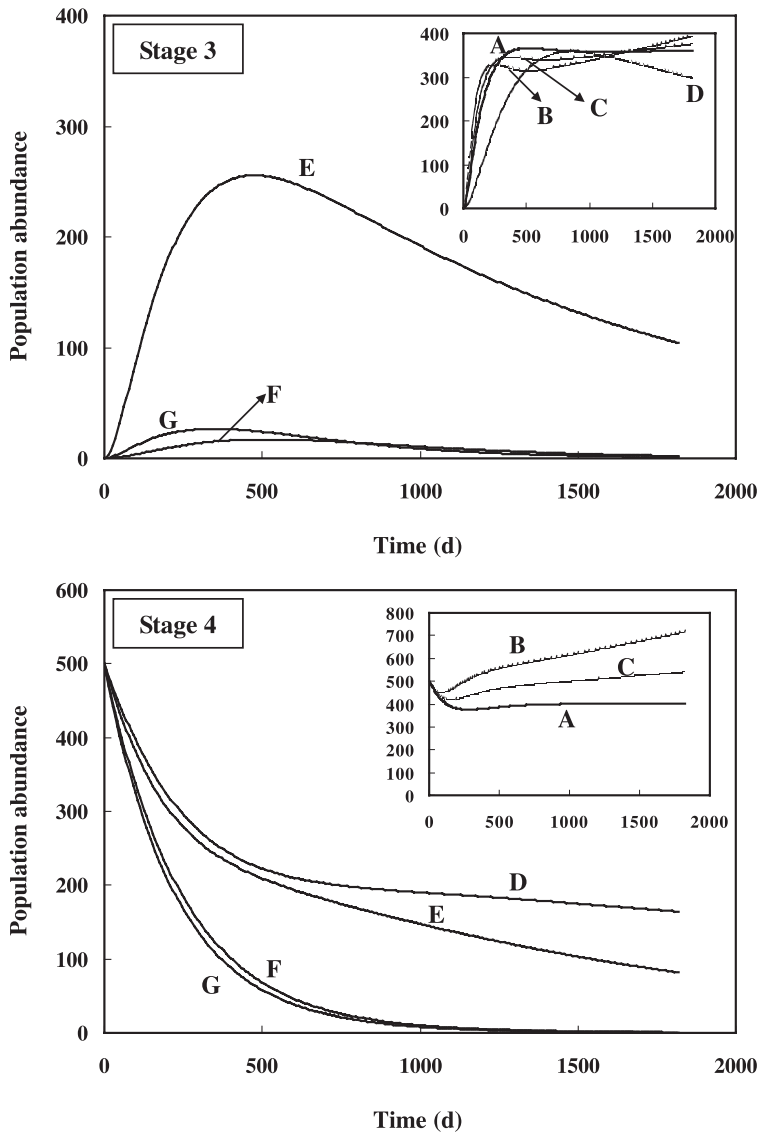


Fig. 5 (continued).

invertebrates exposed to various kinds of metals (Klok and deRoos, 1996; Mauri et al., 2003). To our knowledge, however, no previous study regarding hormetic effect on population level was available even though this phenomenon was widely recognized for individual level. Our results demonstrated that since mortality rates and reproduction rates were negatively affected by Zn exposure, the positive population growth rates for Scenarios B and C were mainly due to the stimulations of individual growth rates (Fig. 3), indicating an increasing in individual growth rate will shorten the retention time in each

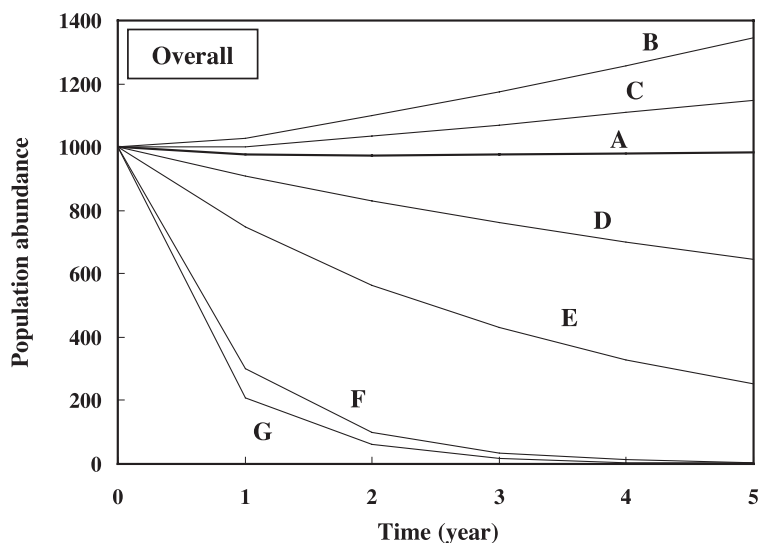


Fig. 5 (continued).

life stage, advance the time to maturity, and hence enlarge the value of growth probability of the population projection matrix.

Simas et al. (2001) proposed the monotonic and sigmoid concentration–response profiles for Cd and Hg on population abundance of the brown shrimp *Crangon crangon*.

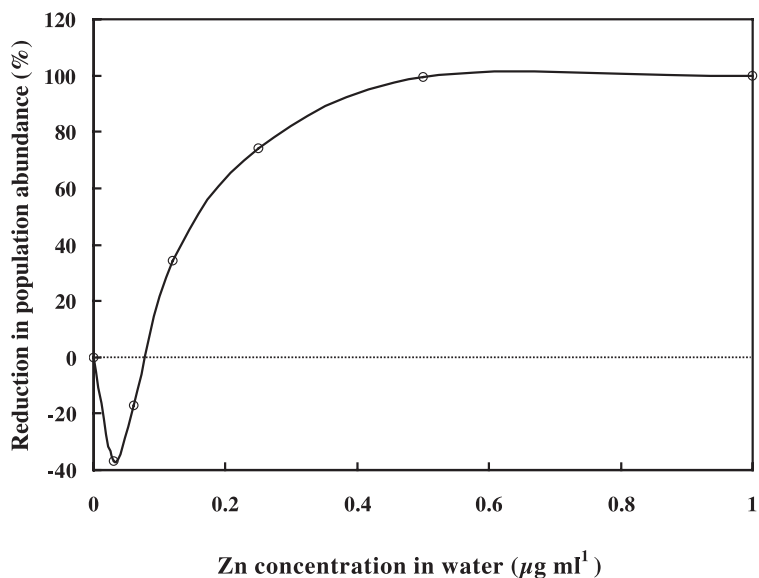


Fig. 6. Concentration–response profile of abalone population exposed to waterborne Zn after a 5-year simulation in that a negative reduction in population abundance indicates a positive population growth rate.



An U-shape concentration–response profile, however, was obtained in the present study (Fig. 6). Such a discrepancy may be due to the target species and chemicals used, or may be resulted from the scale of concentration of the chemicals. In addition, the obtained U-shape concentration–response profile can be also explained on the basis of the Zn hormetic effect found. Lee et al. (1996) reported that maximum Zn concentrations in aquacultural waters in different areas of Taiwan were reported to range from 0.06 to 0.13  $\mu\text{g ml}^{-1}$ . The population abundance of abalone may increase or decrease in these field circumstances according to the concentration–response profile shown in Fig. 6. Consequently, while setting up the ambient water quality criteria and/or identifying remedial goals for contaminated sites, the hormetic effects on both individual and population levels should be taken into consideration.

#### 4. Conclusions

We have linked the population model with the laboratory toxicity data to demonstrate the relationship between individual-level and population-level responses for abalone *H. diversicolor supertexta* exposed to waterborne Zn. We also have considered the time-varying dietary Zn uptake by abalone to predict the overall Zn accumulation in abalone. Specifically, our results show that an increase in individual growth is associated with an increase in the size of population for abalone subject to lower concentration of Zn. In particular, the decline and ultimately localized extinction of abalone population may occur at higher Zn exposure. Our approaches and findings are particularly important when extrapolating laboratory-derived toxicity data to the population-level effects, or when generating the water quality criterion for protection of aquatic species both at individual and population levels. We recommend that future research focuses both on the relationship between Zn concentrations and some key aspects of aquaculture (e.g., harvest time, total biomass, commercial biomass and time required for reaching commercial biomass), and on a more thorough evaluation of the interactions of Zn with toxic metals commonly found in abalone farming sites (e.g., Al, Cu, Pb, Co, As).

#### References

- Appleyard, C.L., Dealeris, J.T., 2001. Modeling growth of the northern quahog, *Mercenaria mercenaria*. J. Shellfish Res. 20, 1117–1125.
- Calabrese, E.J., Baldwin, L.A., 2003. Toxicology rethinks its central belief—Hormesis demands a reappraisal of the way risks are assessed. Nature 421, 691–692.
- Caswell, H., 2001. Matrix Population Models: Construction, Analysis, and Interpretation, 2nd ed. Sinauer Associates, Sunderland, MA, USA.
- Chaumot, A., Charles, S., Flammarion, P., Auger, P., 2003. Ecotoxicology and spatial modeling in population dynamics: an illustration with brown trout. Environ. Toxicol. Chem. 22, 958–969.
- Chen, J.C., Lee, W.C., 1999. Growth of Taiwan abalone *Haliotis diversicolor supertexta* fed on *Gracilaria tenuistipitata* and artificial diet in a multiple-tier basket system. J. Shellfish Res. 18, 627–635.
- Ducrot, V., Pery, A.R.R., Mons, R., Garric, J., 2004. Energy-based modeling as a basis for the analysis of reproductive data with the midge (*Chironomus riparius*). Environ. Toxicol. Chem. 23, 225–231.

- Eggen, R.I.L., Behra, R., Burkhardt-Holm, P., Escher, B.I., Schweigert, N., 2004. Challenges in ecotoxicology. *Environ. Sci. Technol.* 38, 58A–64A.
- Grist, E.P.M., Crane, M., Jones, C., Whitehouse, P., 2003. Estimation of demographic toxicity through the double bootstrap. *Water Res.* 37, 618–626.
- Gross-Sorokin, M.Y., Grist, E.P.M., Cooke, M., Crane, M., 2003. Uptake and depuration of 4-nonylphenol by the benthic invertebrate *Gammarus pulex*: how important is feeding rate? *Environ. Sci. Technol.* 37, 2236–2241.
- Hogstrand, C., Webb, N., Wood, C.M., 1998. Covariation in regulation of affinity for branchial zinc and calcium uptake in freshwater rainbow trout. *J. Exp. Biol.* 201, 1809–1815.
- Kammenga, J., Laskowski, R., 2000. *Demographic in Ecotoxicology*. Wiley, Chichester, UK.
- Klok, C., deRoos, A.M., 1996. Population level consequences of toxicological influences on individual growth and reproduction in *Lumbricus rubellus* (Lumbricidae Oligochaeta). *Ecotoxicol. Environ. Saf.* 33, 118–127.
- Kooijman, S.A.L.M., 1998. Process-Oriented Descriptions of Toxic Effects. In: Schuurmann, G., Markert, B. (Eds.), *Ecotoxicology: Ecological Fundamentals, Chemical Exposures, and Biological Effect*. Wiley, NY, USA, pp. 483–520.
- Kramarz, P., Laskowski, R., 1997. Effect of zinc contamination on life history parameters of a ground beetle. *Poecilus cupreus*. *Bull. Environ. Contam. Toxicol.* 59, 525–530.
- Kuhn, A., Munns, W.R., Serbst, J., Edwards, P., Cantwell, M.G., Gleason, T., Pelletier, M.C., Berry, W., 2002. Evaluating the ecological significance of laboratory response data to predict population-level effects for the estuarine amphipod *Ampelisca abdita*. *Environ. Toxicol. Chem.* 21, 865–874.
- Laskowski, R., 2000. Stochastic and Density-Dependent Models in Ecotoxicology. In: Kammenga, J., Laskowski, R. (Eds.), *Demographic in Ecotoxicology*. Wiley, Chichester, UK, pp. 57–71.
- Laskowski, R., Hopkin, S.P., 1996. Effect of Zn, Cu, Pb, and Cd on fitness in snails (*Helix aspersa*). *Ecotoxicol. Environ. Saf.* 34, 59–69.
- Lee, C.L., Chen, H.Y., Chuang, M.Y., 1996. Use of oyster, *Crassostrea gigas*, and ambient water to assess metal pollution status of the charting coastal area, Taiwan, after the 1986 green oyster incident. *Chemosphere* 33, 2505–2532.
- Liao, C.M., Lin, M.C., 2001. Toxicokinetics and acute toxicity of waterborne zinc in abalone (*Haliotis diversicolor supertexta* Lischke). *Bull. Environ. Contam. Toxicol.* 66, 597–602.
- Liao, C.M., Ling, M.P., 2004. Probabilistic risk assessment of abalone *Haliotis diversicolor supertexta* exposed to waterborne zinc. *Environ. Pollut.* 127, 217–227.
- Liao, C.M., Chen, B.C., Lin, M.C., Chiu, H.M., Chou, Y.H., 2002a. Coupling toxicokinetics and pharmacodynamics for predicting survival of abalone (*Haliotis diversicolor supertexta*) exposed to waterborne zinc. *Environ. Toxicol.* 17, 478–486.
- Liao, C.M., Lin, M.C., Chen, J.S., Chen, J.W., 2002b. Linking biokinetics and consumer-resource dynamics of zinc accumulation in pond abalone *Haliotis diversicolor supertexta*. *Water Res.* 36, 5102–5112.
- Liao, C.M., Chen, B.C., Tsai, J.W., Chen, J.W., Ling, M.P., Chou, Y.H., 2004. A parsimonious AUC-based biokinetic method to estimate relative bioavailable zinc to abalone *Haliotis diversicolor supertexta*. *Aquaculture* 232, 425–440.
- Martinez-Ponce, D.R., Searcy-Bernal, R., 1998. Grazing rates of red abalone (*Haliotis rufescens*) postlarvae feeding on the benthic diatom *Navicula incerta*. *J. Shellfish Res.* 17, 627–630.
- Mauri, M., Baraldi, E., Simonini, R., 2003. Effects of zinc exposure on the polychaete *Dinophilus gyrociliatus*: a life-table response experiment. *Aquat. Toxicol.* 65, 93–100.
- Muyssen, B.T.A., Janssen, C.R., 2002. Tolerance and acclimation to zinc of *Ceriodaphnia dubia*. *Environ. Pollut.* 117, 301–306.
- Renner, R., 2004. Redrawing the dose–response curve. *Environ. Sci. Technol.* 38, 90A–95A.
- Shepherd, S.A., 1998. Studies on southern Australian abalone (genus *Haliotis*): XIX. Long-term juvenile mortality dynamics. *J. Shellfish Res.* 17, 813–825.
- Simas, T.C., Ribeiro, A.P., Ferreira, J.G., 2001. Shrimp—a dynamic model of heavy-metal uptake in aquatic macrofauna. *Environ. Toxicol. Chem.* 20, 2649–2656.
- Steinarsson, A., Imsland, A.K., 2003. Size dependent variation in optimum growth temperature of red abalone (*Haliotis rufescens*). *Aquaculture* 224, 353–362.
- Tsai, J.W., Chou, Y.H., Chen, B.C., Liang, H.M., Liao, C.M., 2004. Growth toxicity bioassays of abalone *Haliotis diversicolor supertexta* exposed to waterborne zinc. *Bull. Environ. Contam. Toxicol.* 72, 70–77.

- US EPA, 1991. Summary report on issues in ecological risk assessment. EPA/625/3-91/018F, US Environmental Protection Agency, Washington, DC.
- Van Straalen, N.M., Kammenga, J.E., 1998. Assessment of ecotoxicity at the population level using demographic parameters. In: Schuurmann, G., Markert, B. (Eds.), *Ecotoxicology: Ecological Fundamentals, Chemical Exposures, and Biological Effect*. Wiley, NY, USA, pp. 621–644.
- Wang, W.X., Ke, C., 2002. Dominance of dietary intake of cadmium and zinc by two marine predatory gastropods. *Aquat. Toxicol.* 56, 153–165.
- Yang, H.S., Ting, Y.Y., 1984. Studies on the availability of the abalone *Haliotis diversicolor supertexta* Lischke) culture in southern Taiwan. *Bull. Taiwan Fish. Res. Inst.* 37, 145–154.
- Yang, H.S., Ting, Y.Y., 1986. Artificial propagation and culture of abalone (*Haliotis diversicolor supertexta* Lischke). *Bull. Taiwan Fish. Res. Inst.* 40, 195–201.